

Acute Stroke Paper Supplemental Results

Eckhard Schlemm

Results

Missing data

Tab S1 reports details about the clinical outcome parameters collected during the study.

ID	0_FM	0_Gripstrength_ratio	0_NIHSS	1_FM	1_Gripstrength_ratio	1_NIHSS	12_FM	12_Gripstrength_ratio	12_NIHSS	3_FM	3_Gripstrength_ratio	3_NIHSS
3	•		•	•		•	•		•	•		•
5				•	•	•	•		•	•		•
7	•	•	•	•	•	•	•	•	•	•	•	•
9	•		•	•	•	•	•	•	•	•	•	•
12	•	•	•	•	•	•	•	•	•	•	•	•
13	•	•	•	•	•	•	•	•	•	•	•	•
14	•	•	•	•	•	•	•	•	•	•	•	•
15	•	•	•	•	•	•	•	•	•	•	•	•
16	•	•	•	•	•	•	•	•	•	•	•	•
20	•		•	•	•	•	•		•	•	•	•
22	•	•	•	•	•	•	•	•	•	•	•	•
23	•	•	•	•	•	•					•	•
24	•	•	•	•	•	•	•	•	•	•	•	•
25	•	•	•	•	•	•	•	•	•	•	•	•
26	•	•	•	•	•	•	•	•	•	•	•	•
30	•	•	•	•	•	•	•	•	•	•	•	•
32	•	•	•	•	•	•	•	•	•	•	•	•
33	•	•	•	•	•	•	•	•	•	•	•	•
35	•	•	•	•	•	•	•	•	•	•	•	•
36	•	•	•	•	•	•	•	•	•	•	•	•
43	•	•	•	•	•	•	•	•	•	•	•	•
44	•	•	•	•	•	•	•	•	•	•	•	•
45	•	•	•	•	•	•	•	•	•	•	•	•
46	•	•	•	•	•	•	•	•	•	•	•	•
47	•	•	•	•	•	•	•	•	•	•	•	•
51	•	•	•	•	•	•	•	•	•	•	•	•
52	•	•	•	•	•	•	•	•	•	•	•	•
53	•	•	•	•	•	•				•	•	•

ID	0_FM	0_Gripstrength_ratio	0_NIHSS	1_FM	1_Gripstrength_ratio	1_NIHSS	12_FM	12_Gripstrength_ratio	12_NIHSS	3_FM	3_Gripstrength_ratio	3_NIHSS
54	•	•	•	•	•	•	•	•	•	•	•	•
55	•		•	•	•	•	•	•	•	•	•	•

Details of missing clinical data by subject, timepoint and testing modality.

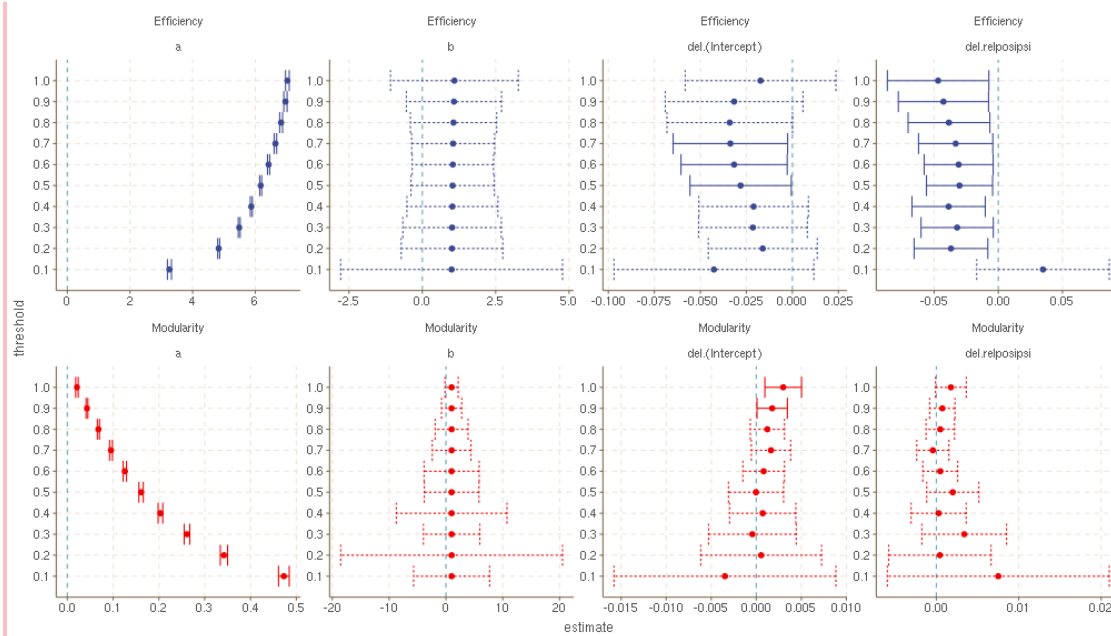
Global graph parameters

In the main text it was established that global network measures change after stroke and that the change is significantly more pronounced in ipsilesional hemispheres compared to contralesional hemispheres. For the analysis there, structural brain networks were not thresholded, retaining their original edge density of $\approx 95\%$. Here we present supplementary results about the effects of time and lesion status on global graph parameters if connectomes are thresholded to a range of common network densities ranging from 10% to 90%. For each subject, a sparsity mask was constructed from the brain network from the first available visit (t_{3-5d} in 27 patients, t_{1m} in 3 patients) by only retaining the $k\%$ strongest connections and binarizing the result. This sparsity mask was then multiplied edgewise with the connectomes of the same subject at all later time points, thus eliminating weak, potentially spurious connections. Global graph parameters efficiency, clustering, modularity and assortativity were computed for thresholded networks using the Brain Connectivity Toolbox as before and analysed using the non-linear mixed effects regression model

$$y_t \sim a + \Delta(1 - \exp(-bt)).$$

Sensitivity analysis for the effects of time and lesion status on global graph parameters

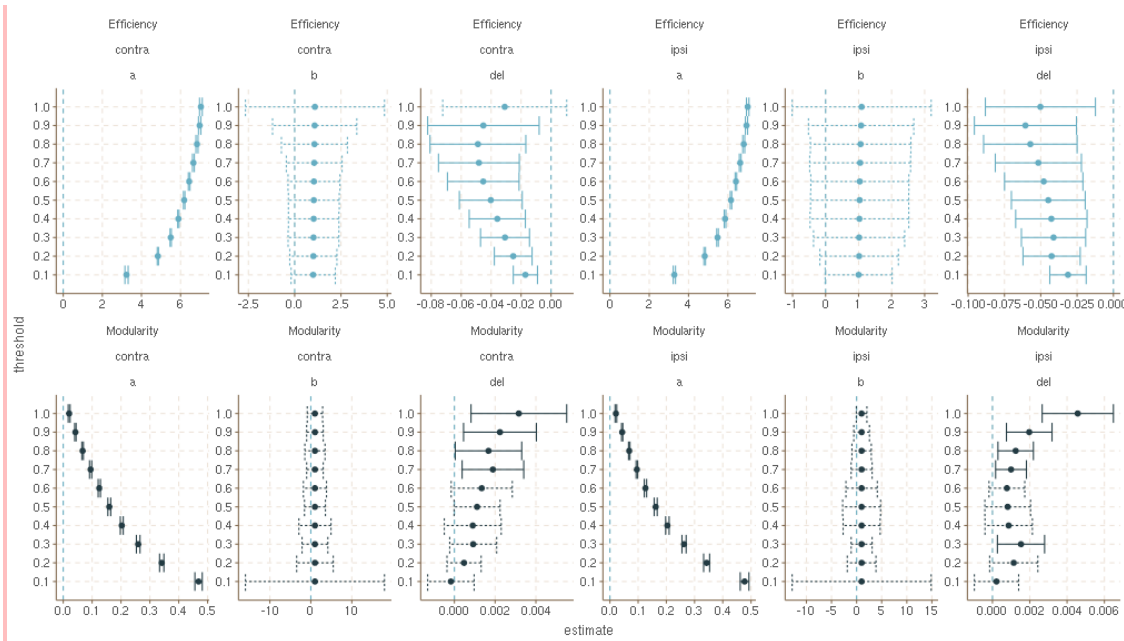
Differences in the time course of GGPs between ipsi- and contralesional hemispheres were assessed by allowing different values of Δ in the two groups. Results are displayed visually in FigX.



Results of non-linear mixed-effects regression modelling of global graph parameters jointly in stroke and intact hemispheres for different network densities. Dots indicate point estimates, bars 95% confidence intervals. Solid lines indicate intervals not containing zero.

The dependence of the global graph metrics on network density is reflected in the intercept model parameter a which indicates a rapid decline of both efficiency and clustering and a marked increase in modularity in very sparse networks. Assortativity is negative for all thresholds with a minimum occurring at a density of 50%. An excess decline in ipsilesional efficiency and clustering, as measured by Δ_{relpos} is statistically significant at all but the smallest thresholds. There is no significant difference in the increase in modularity at any threshold. The nuisance parameter b quantifying the rate of change over time is numerically stable across thresholds and not significantly different from zero for all considered GGPs.

The time course of GGPs was also quantified and analysed in stroke and intact hemispheres separately (FigX).



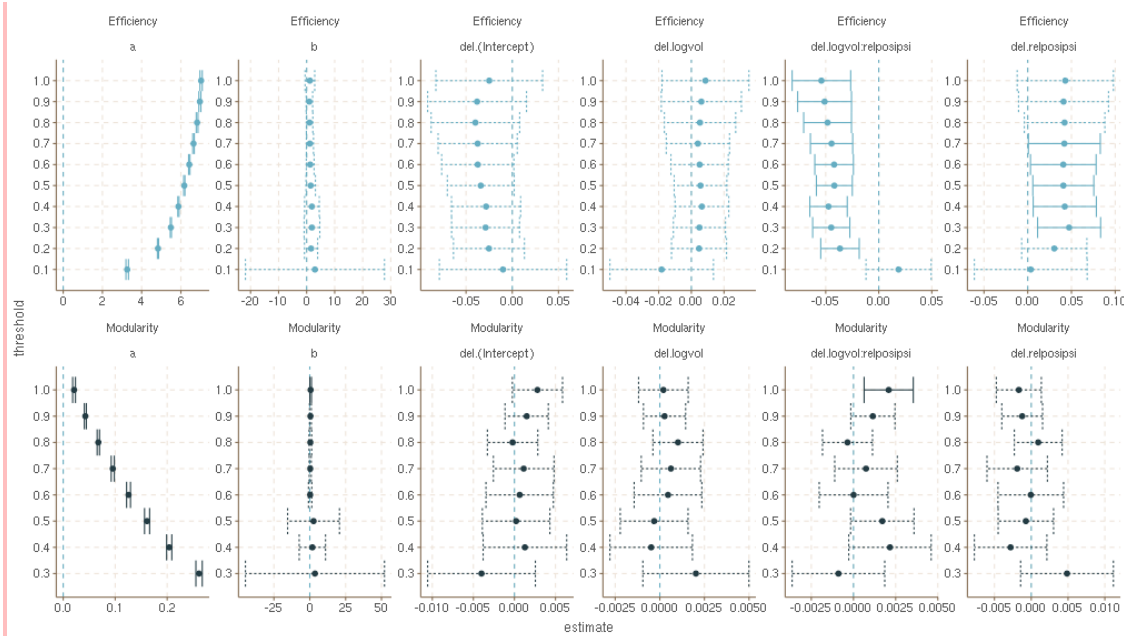
Results of non-linear mixed-effects regression modelling of global graph parameters separately in stroke and intact hemispheres for different network densities. Dots indicate point estimates, bars 95% confidence intervals. Solid lines indicate intervals not containing zero.

It is seen that decline in efficiency and clustering, as well as increase in modularity are significant across threshold both ipsi- and contralesionally with a numerically larger effect in hemispheres directly affected by stroke, consistent with the interaction analysis above.

Effect of numerical connectivity on global graph parameters

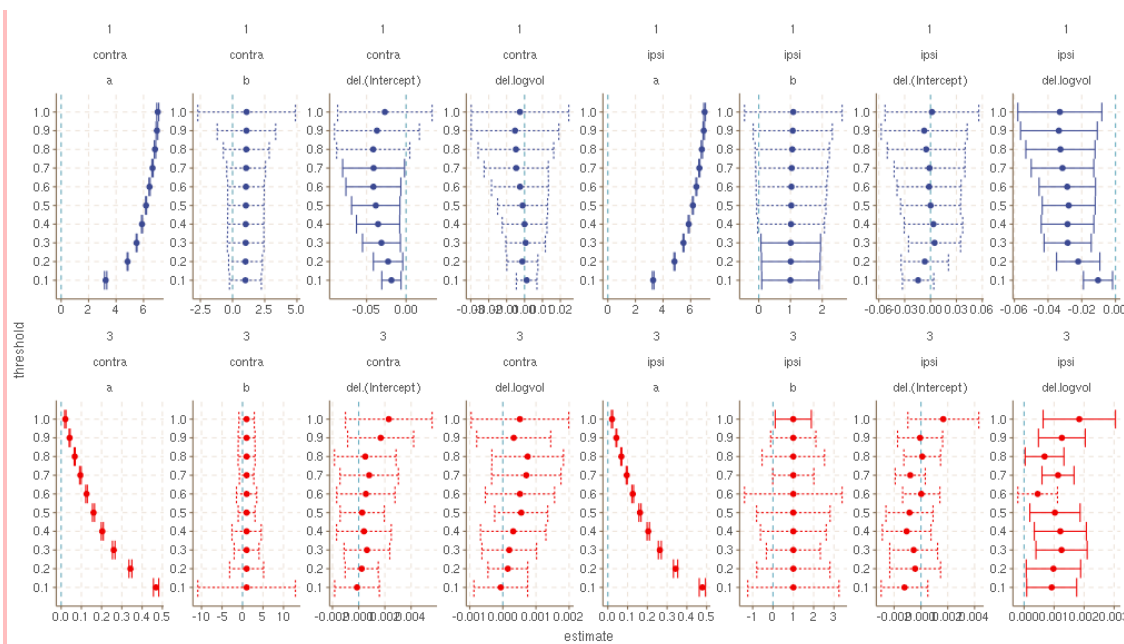
Sensitivity analysis for the effects of lesion volume on global network measures

In the main text it is shown that lesion volume modulates the change in global network architecture over time in stroke but not intact hemispheres. FigX reports a sensitivity analysis for the influence of network density on this effect.



Results of non-linear mixed-effects regressions modelling the effect of lesion volume on change of global graph parameters jointly in stroke and intact hemispheres for different network densities. Dots indicate point estimates, bars 95% confidence intervals. Solid lines indicate intervals not containing zero.

It is seen that the interacting effects of lesion volume and lesion status on structural network change (model parameter Δ) persist across thresholds for global efficiency, clustering and modularity. Subgroup analysis for ipsi- and contralesional hemispheres are presented in FigX.



Results of non-linear mixed-effects regressions modelling the effect of lesion volume on change of global graph parameters separately in stroke and intact hemispheres for different network densities. Dots indicate point estimates, bars 95% confidence intervals. Solid lines indicate intervals not containing zero.

Consistent with the joint analysis, there is a significant effect of lesion volume on topological network change in ipsilesional hemispheres across network densities. There is no significant effect of lesion volume on topological network change in contralesional hemispheres at any network density.

Local graph parameters

Time course of local network change.

In the main text, 8 brain regions with different temporal profiles of local graph measures between ipsi- and contralesional hemispheres as well as 21 regions with a significant decline of local network integrity in stroke hemispheres have been identified. Fig S1.5 shows the timecourse of strength, local efficiency and local clustering in those regions.

Too long -- omitted

Time course of local graph parameters in selected ROIs.

Association between lesion volume and local network change.

Change in ipsilesional global network architecture is modulated by lesion volume. In this section we provide details about the modulation of change in local network by lesion volume. Tab SX lists ROIs with a significant interaction between lesion volume and lesion status on the decline of local network integrity.

temp			
node	clustering	efficiency	strength
postcentral	1.03e-01 +/- 1.60e-02, p=9.15e-10		
precentral	1.00e-01 +/- 1.60e-02, p=2.79e-09		3.50e+00 +/- 7.04e-01, p=1.52e-06
inferiortemporal	1.09e-01 +/- 2.54e-02, p=3.03e-05	9.09e-02 +/- 1.70e-02, p=2.66e-07	
parstriangularis	6.58e-02 +/- 1.76e-02, p=2.47e-04		4.41e+00 +/- 9.05e-01, p=2.39e-06
parsopercularis	8.09e-02 +/- 1.68e-02, p=2.91e-06		
insula	7.69e-02 +/- 1.82e-02, p=3.88e-05	5.94e-02 +/- 1.25e-02, p=3.77e-06	
fusiform	1.13e-01 +/- 2.68e-02, p=4.01e-05	1.04e-01 +/- 2.23e-02, p=5.42e-06	5.35e+00 +/- 1.29e+00, p=5.32e-05
rostralmiddlefrontal	7.13e-02 +/- 1.75e-02, p=6.98e-05	6.15e-02 +/- 1.45e-02, p=3.38e-05	2.50e+00 +/- 7.73e-01, p=1.42e-03
superiortemporal	7.55e-02 +/- 2.08e-02, p=3.59e-04	5.67e-02 +/- 1.39e-02, p=6.88e-05	

node	clustering	efficiency	strength
precuneus	8.16e-02 +/- 2.52e-02, p=1.44e-03	6.66e-02 +/- 1.69e-02, p=1.16e-04	2.55e+00 +/- 7.03e-01, p=3.64e-04
superiorparietal	5.63e-02 +/- 1.80e-02, p=2.00e-03	4.00e-02 +/- 1.13e-02, p=4.93e-04	
superiorfrontal	6.38e-02 +/- 1.88e-02, p=8.58e-04	4.72e-02 +/- 1.37e-02, p=7.12e-04	1.56e+00 +/- 7.40e-01, p=3.59e-02
thalamus	6.89e-02 +/- 2.14e-02, p=1.54e-03	4.77e-02 +/- 1.44e-02, p=1.09e-03	1.24e+00 +/- 6.23e-01, p=4.87e-02
middletemporal	6.43e-02 +/- 2.11e-02, p=2.60e-03	4.50e-02 +/- 1.37e-02, p=1.25e-03	
isthmuscingulate	6.57e-02 +/- 2.36e-02, p=5.85e-03	5.10e-02 +/- 1.57e-02, p=1.38e-03	1.61e+00 +/- 6.68e-01, p=1.71e-02
lateraloccipital	6.57e-02 +/- 2.74e-02, p=1.77e-02	6.20e-02 +/- 2.20e-02, p=5.36e-03	3.49e+00 +/- 1.10e+00, p=1.83e-03
caudalanteriorcingulate	5.92e-02 +/- 1.95e-02, p=2.79e-03	4.27e-02 +/- 1.63e-02, p=9.42e-03	
posteriorcingulate	6.54e-02 +/- 2.33e-02, p=5.45e-03	4.67e-02 +/- 1.87e-02, p=1.32e-02	
paracentral	5.19e-02 +/- 1.90e-02, p=6.83e-03	4.64e-02 +/- 1.65e-02, p=5.57e-03	2.65e+00 +/- 1.13e+00, p=1.98e-02
rostralanteriorcingulate	7.77e-02 +/- 3.22e-02, p=1.70e-02		
frontalpole	1.21e-01 +/- 5.09e-02, p=1.86e-02		
medialorbitofrontal			4.31e+00 +/- 1.84e+00, p=2.02e-02
parsorbitalis	3.82e-02 +/- 1.74e-02, p=2.94e-02		

Restricting the analysis to ipsilesional ROIs, Tab SX reports the effects of lesion volume and local network change in hemispheres directly affected by stroke.

node	clustering	efficiency	strength
rostralmiddlefrontal	-7.14e-02 +/- 1.66e-02, p=4.92e-05	-6.08e-02 +/- 1.30e-02, p=1.15e-05	-2.50e+00 +/- 6.44e-01, p=2.14e-04
precentral	-6.41e-02 +/- 1.59e-02, p=1.29e-04	-5.80e-02 +/- 1.26e-02, p=1.55e-05	-3.17e+00 +/- 6.81e-01, p=1.28e-05
postcentral	-6.74e-02 +/- 1.54e-02, p=3.66e-05	-5.89e-02 +/- 1.27e-02, p=1.32e-05	
superiortemporal	-6.64e-02 +/- 1.86e-02, p=6.12e-04	-5.32e-02 +/- 1.27e-02, p=7.04e-05	
parstriangularis	-5.06e-02 +/- 1.80e-02, p=6.29e-03		-3.60e+00 +/- 8.80e-01, p=1.05e-04
paracentral	-7.67e-02 +/- 1.89e-02, p=1.15e-04	-6.64e-02 +/- 1.63e-02, p=1.12e-04	-3.35e+00 +/- 1.13e+00, p=4.02e-03
caudalanteriorcingulate	-7.59e-02 +/- 1.99e-02, p=2.66e-04	-6.39e-02 +/- 1.63e-02, p=1.92e-04	-2.48e+00 +/- 8.24e-01, p=3.49e-03
lateraloccipital	-6.02e-02 +/- 1.80e-02, p=1.30e-03	-5.17e-02 +/- 1.38e-02, p=3.30e-04	-2.33e+00 +/- 7.36e-01, p=2.20e-03
fusiform	-8.20e-02 +/- 2.41e-02, p=1.04e-03	-7.31e-02 +/- 1.99e-02, p=4.44e-04	-3.60e+00 +/- 1.08e+00, p=1.29e-03
insula	-6.03e-02 +/- 1.82e-02, p=1.39e-03	-4.80e-02 +/- 1.32e-02, p=4.77e-04	-1.72e+00 +/- 5.76e-01, p=3.79e-03
thalamus	-5.22e-02 +/- 1.86e-02, p=6.22e-03	-4.18e-02 +/- 1.17e-02, p=6.21e-04	-1.55e+00 +/- 4.53e-01, p=9.62e-04
superiorfrontal	-5.84e-02 +/- 1.73e-02, p=1.17e-03	-4.20e-02 +/- 1.22e-02, p=9.11e-04	
inferiortemporal	-5.87e-02 +/- 2.08e-02, p=6.03e-03	-4.68e-02 +/- 1.46e-02, p=1.98e-03	

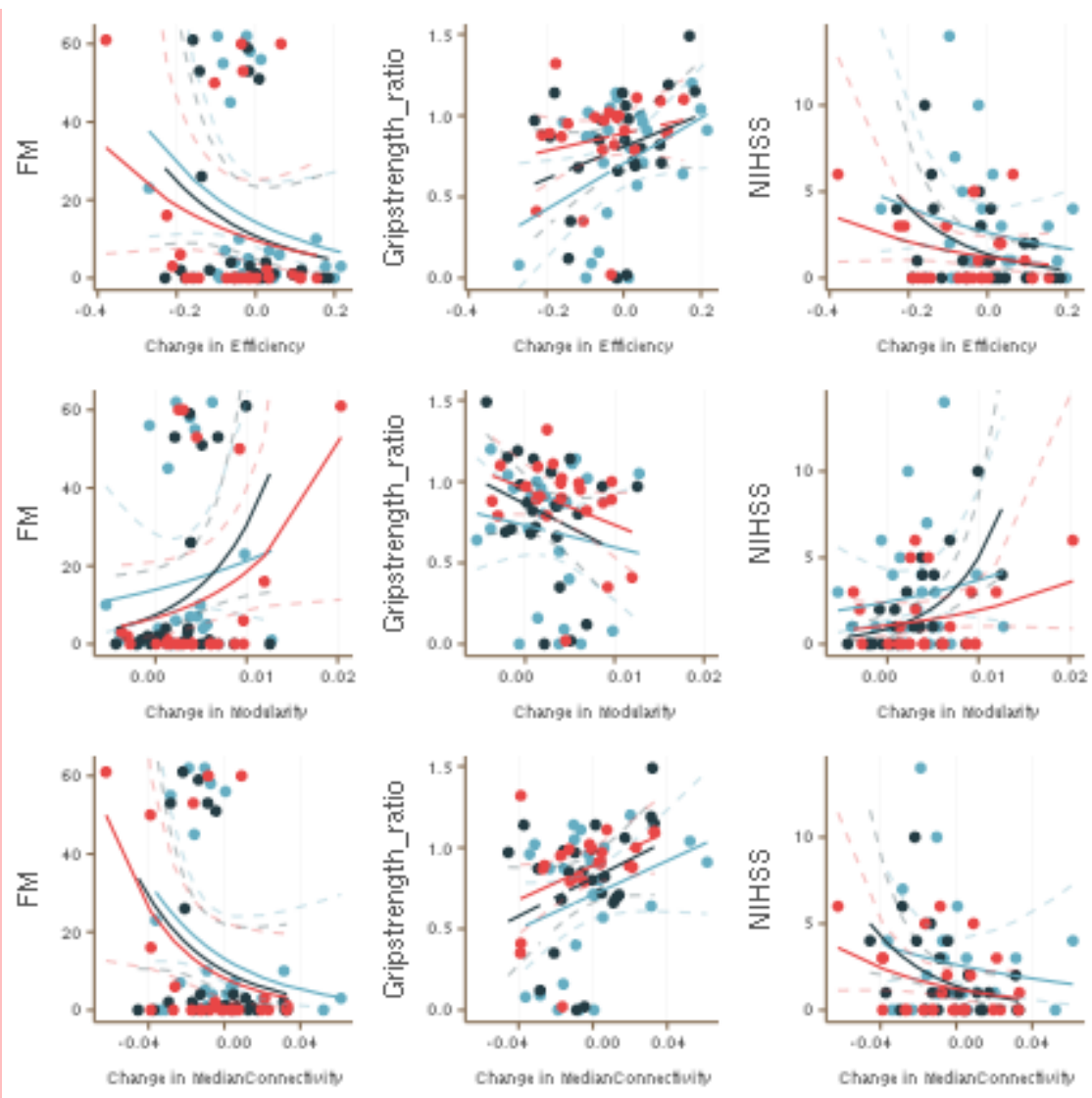
node	clustering	efficiency	strength
superiorparietal	-5.06e-02 +/- 1.64e-02, p=2.78e-03	-3.48e-02 +/- 1.11e-02, p=2.39e-03	
pericalcarine	-6.70e-02 +/- 2.27e-02, p=4.12e-03	-5.92e-02 +/- 2.14e-02, p=6.96e-03	
supramarginal	-5.01e-02 +/- 1.71e-02, p=4.42e-03	-3.77e-02 +/- 1.30e-02, p=4.99e-03	
posteriorcingulate	-5.88e-02 +/- 2.10e-02, p=6.44e-03	-4.51e-02 +/- 1.61e-02, p=6.38e-03	
temporalpole	-6.52e-02 +/- 2.51e-02, p=1.12e-02	-5.87e-02 +/- 2.10e-02, p=6.48e-03	
isthmuscingulate	-4.88e-02 +/- 2.20e-02, p=2.97e-02	-3.70e-02 +/- 1.55e-02, p=1.94e-02	
parahippocampal		-4.25e+00 +/- 1.84e+00, p=2.32e-02	
middletemporal	-4.39e-02 +/- 2.08e-02, p=3.80e-02	-3.36e-02 +/- 1.57e-02, p=3.58e-02	
caudalmiddlefrontal	-3.76e-02 +/- 1.78e-02, p=3.76e-02		
precuneus	-4.68e-02 +/- 2.28e-02, p=4.35e-02		

Model parameters (estimate +/- standard error) obtained from fitting the exponential model (1) to temporal profiles of local graph measures in individual ipsilesional ROIs. Total change Δ is modelled as a linear function of log lesion volume.. Standard errors and p -values result from non-linear mixed-effects regressions fit using the R package nlme. ROIs without a significant effect of lesion volume on local network change are not shown.

Associations between network change and clinical outcome.

Global graph measures

In the main text, an association between change in global network measures and residual symptom burden and motor function was established. Fig S2 provides visualisations of the cross-sectional associations at three time points after stroke.



Relation between change in global network measures and clinical outcome parameters in the subacute (3-5d after stroke, red) and chronic stages (3m after stroke, orange; 12m after stroke, grey). Abscissæ represent network change. Solid lines indicate predicted mean clinical outcome under quasi-Poisson (NIHSS, FM) or Gaussian (grip strength) models, fit separately for the three time points. Dashed lines represent upper and lower 95% confidence band for the predicted mean.

Local graph measures

For each node, the association of decline in weighted degree, efficiency until one, three and twelve months after stroke and clustering with grip strength, NIHSS and FM scores was assessed by two-stage linear and quasi-Poisson regression.

node	FM_stren gth	Gripstrength_ratio_str ength	NIHSS_stren gth	vol_FM_stren gth	vol_Gripstrength_ratio_st rength	vol_NIHSS_stre ngth
------	-----------------	---------------------------------	--------------------	---------------------	-------------------------------------	------------------------

node	FM_stren gth	Gripstrength_ratio_str ength	NIHSS_stren gth	vol_FM_stren gth	vol_Gripstrength_ratio_st rengh	vol_NIHSS_stre ngth
caudalanteriorcing ulate					-0.02 +/- 0.01, p=0.0049	
cuneus	-0.03 +/- 0.01, p=0.0083		-0.04 +/- 0.01, p=0.0002	-0.03 +/- 0.01, p=0.0307		-0.03 +/- 0.01, p=0.0019
middletemporal	-0.15 +/- 0.05, p=0.0046	0.03 +/- 0.01, p=0.0148	-0.12 +/- 0.04, p=0.0034	-0.13 +/- 0.05, p=0.0193		-0.10 +/- 0.04, p=0.0269
paracentral	-0.12 +/- 0.03, p=0.0003	0.02 +/- 0.01, p=0.0023	-0.09 +/- 0.02, p=0.0001	-0.10 +/- 0.03, p=0.0026	0.02 +/- 0.01, p=0.0251	-0.07 +/- 0.02, p=0.0021
parsopercularis		0.02 +/- 0.00, p=0.0002	-0.03 +/- 0.01, p=0.0189		0.01 +/- 0.00, p=0.0160	
parstriangularis	-0.09 +/- 0.02, p=0.0003	0.03 +/- 0.01, p=0.0000	-0.07 +/- 0.02, p=0.0018	-0.08 +/- 0.04, p=0.0301	0.03 +/- 0.01, p=0.0003	
pericalcarine	-0.05 +/- 0.02, p=0.0161	0.01 +/- 0.00, p=0.0352	-0.05 +/- 0.02, p=0.0044	-0.04 +/- 0.02, p=0.0325		-0.04 +/- 0.02, p=0.0103
posteriorcingulate	-0.09 +/- 0.04, p=0.0376		-0.09 +/- 0.03, p=0.0046			-0.07 +/- 0.03, p=0.0325
precentral		0.02 +/- 0.01, p=0.0065	-0.05 +/- 0.02, p=0.0153			
rostralanteriorcing ulate	0.06 +/- 0.03, p=0.0369	-0.02 +/- 0.01, p=0.0174	0.06 +/- 0.02, p=0.0210	0.06 +/- 0.03, p=0.0479	-0.01 +/- 0.01, p=0.0216	0.05 +/- 0.02, p=0.0282
superiorparietal		0.03 +/- 0.01, p=0.0280				
superiortemporal	-0.17 +/- 0.05, p=0.0008	0.04 +/- 0.01, p=0.0002	-0.11 +/- 0.04, p=0.0027	-0.16 +/- 0.07, p=0.0191	0.03 +/- 0.01, p=0.0374	
temporalpole	-0.08 +/- 0.02, p=0.0007	0.02 +/- 0.01, p=0.0038	-0.06 +/- 0.02, p=0.0005	-0.07 +/- 0.03, p=0.0130		-0.05 +/- 0.02, p=0.0176
thalamus	-0.16 +/- 0.04, p=0.0000	0.04 +/- 0.01, p=0.0007	-0.10 +/- 0.03, p=0.0037	-0.15 +/- 0.05, p=0.0031	0.02 +/- 0.01, p=0.0489	

Regression coefficients (estimate +/- standard error) on the link scale between change in local network measures and clinical outcome from joint two-stage regressions across subacute and chronic stages. In the case of FM and NIHSS scores, quasi-Poisson regressions with a \log -link are used; in the case of relative grip strength a Gaussian regression with identity link is used. ROIs without a significant association between network change and clinical outcome are not shown.